

Time constants in the ionosphere from neural network models

Martin Friedrich^{*}, Martin Fankhauser

Graz University of Technology, Inffeldgasse 12, A-8010 Graz, Austria

Available online 29 September 2011

Abstract

Neural network (NN) models for the low latitude and the polar ionosphere from the *D*- to the *F*-region were developed which are based on incoherent scatter radar data from Arecibo and EISCAT Svalbard, respectively. The various geophysical input parameters defining the NN are not only the ones that represent the time one wants to predict, but also the geophysical conditions prior to the time of the prediction. The optimum length of these preceding periods are derived for the two models are different, but a period of 60 days is a compromise acceptable for both latitudes. Furthermore from the Arecibo data time constants of electron density decay after sundown are derived which – arguably – are also relevant elsewhere, including the polar latitudes. Whereas at all altitudes the electron densities decay exponentially after sundown, below 300 km there is an additional variation with solar zenith angle.

© 2011 COSPAR. Published by Elsevier Ltd. All rights reserved.

Keywords: Ionosphere; Arecibo; Svalbard; Neural network; Time constants

1. Introduction

Due to the larger background density and the resulting short lifetime of free electrons the lower ionosphere (covering the *D*- and *E*-regions) in general is controlled by the geophysical condition prevailing at the time, i.e. primarily solar zenith angle and solar activity. At higher altitudes, however, the number density of free electrons also depends in the geophysical “history”, notably on the geomagnetic disturbance, the solar activity and indeed the electron density itself a few hours to a few days prior, but also transport can play a role. Using a large data base of electron densities from the incoherent scatter radars at Arecibo and on Svalbard we investigate which time periods and time constants are important to describe the ionosphere above the altitudes where one usually assumes steady-state conditions.

2. Lifetime of free electrons

When transport effects can be neglected the free electrons of the ionosphere are maintained by continuous ion-

isation from various sources. Once these sources are switched off (after sundown, or more rapidly during an eclipse) free electrons disappear either by recombination forming neutrals or by attachment to neutrals forming negative ions (or charged aerosols). In a real ionosphere at night electron densities do not disappear completely, but – depending on the altitude – reach a new equilibrium of much smaller densities. Fig. 1 shows the (logarithmic) median electron densities of all day and night profiles from the Arecibo incoherent scatter radar (all online data from 1966 to 2002 inclusive). The median daytime zenith angle is 64.5° and 136.4° for the night conditions. Clearly the night values are always smaller than those of daytime, but the factor between day and night varies considerably with altitude.

There are three main causes for the existence of electron densities at night:

- (1) residual ionising radiation (solar Lyman- α and $-\beta$ scattered in the geocorona, galactic cosmic rays, stellar X-rays, particle drizzle),
- (2) finite velocity of recombination and electron-neutral attachment, and,
- (3) transport from the illuminated part of the Earth to the dark side.

^{*} Corresponding author.

E-mail address: martin.friedrich@tugraz.at (M. Friedrich).

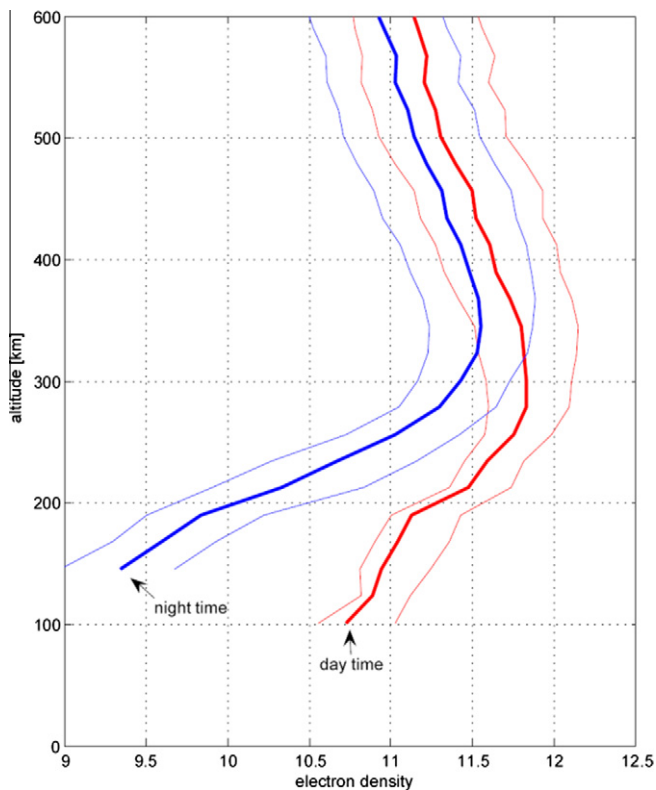


Fig. 1. Median electron densities with upper and lower quartiles above Arecibo for day and night.

We will concentrate on the first two processes, although transport may also play a role. Fig. 2 shows the idealised variation of electron densities during a day at various altitudes for median geophysical conditions. The figure is due to an empirical model that is built using the incoherent scatter data from the Arecibo radar. The model is based on a neural network (NN) incorporating about 100,000 electron density profiles with a total of 1.5 million data points. It uses the inputs a_p , $F_{10.7}$, daily integrated insolation and solar zenith angle χ , all both at the time of the measurement as well as averaged over a lead time (see later). Both the altitude and the pressure with each electron density value entered the model with its three hidden layers. By a simple definition, a NN is a multi-dimensional, weighted interpolation procedure; for an introduction to neural networks see, e.g. Zell and Mamier (2005). Typically this model predicts electron densities with an rms error factor of 2 or better (Fankhauser, 2010). The curves are for various constant altitudes above 150 km and higher, i.e. above the altitude where most measured profiles typically begin. The model was not only trained with χ , but implicitly also with local time ($\cos \chi$ – as a measure of solar input – integrated over the 11 preceding hours) as one of the input parameters. Therefore results are not necessarily symmetric to local noon or local midnight. The brief rise at sunset is presumably an artefact, a though at sunrise such a feature is predicted at lower altitudes due to photodetachment of electrons from negative ions (Ogawa and Shimazaki, 1975; Kazil, 2002). At 150 km the variation

is largely symmetrical about noon and midnight, i.e. throughout the day apparently dominated by the solar zenith angle. Whereas at higher altitudes (≥ 300 km) during the sunlit hours the variation is still largely symmetric to local noon, it is not symmetric to midnight, but the electron densities clearly decay exponentially after sunset. The divider between day and night is the solar zenith angle at which at a particular altitude the Sun is above the horizon, or – arguably more importantly – above the ozone layer. An effective altitude of this layer of 25 km yields a day–night limit of 98° for the D-region, a value found confirmed in ionospheric data (Stauning, 1996). This ozone-determined horizon is chiefly relevant for the chemistry of negative ions which are only found in the nocturnal lower ionosphere. At 800 km this limiting zenith angle for full night-time conditions increases to 117° . Residual solar UV (Lyman- α and - β) is due to scattering in the geocorona and is therefore a function solar zenith angle beyond sunset. According to the theoretical calculation by Strobel et al. (1974) these fluxes decrease by almost a factor of ten between 100° and 180° . To illustrate the expected night-time behaviour in Fig. 3 measured electron densities from the Arecibo radar (all seasons and solar activities) are plotted against hour after sunset and *vs.* solar zenith angle (i.e. $>109^\circ$ at 400 km). The values shown are the averages in bins of 10° by 20 min. Clearly the electron densities at larger zenith angles are smallest and they also steadily decrease after sundown. The simplest function by which one can obtain the dependencies is to fit an rms-plane to these electron density values which yields gradients with time after sunset and with solar zenith angle. The arrow is the resultant of the two gradients, i.e. with time and zenith angle beyond sunset (in percent per hour and percent per deg, respectively).

The results indicated in the figure are not very pronounced because electron densities of all seasons, solar activities and magnetic disturbances were used and hence the reference values at the beginning of the night vary largely. We therefore apply this procedure to the values from the NN model for median geophysical conditions (as for Fig. 2) which we consider to represent a weighted mean over all geophysical conditions. The resulting dependences on time after sunset, and (nocturnal) solar zenith as a function of altitude are depicted in Fig. 4. Clearly up to 250 km the solar zenith angle controls the electron density, whereas above 250 km the time after sunset becomes more important. The altitude where the decay is fastest (430 km) is close to the 370 km found by Sharma et al. (2010) at a comparable latitude in the Indian Zone. These authors formed the ratio between electron densities during a solar eclipse and densities on a reference day. However, the magnitude of the eclipse depletion of 70% cannot be directly compared to the present decay maximum of 17% per hour because of the different references (start values), namely the already small values at the beginning of full night-time conditions in the present case *vs.* the full daylight densities in the case of the eclipse study.

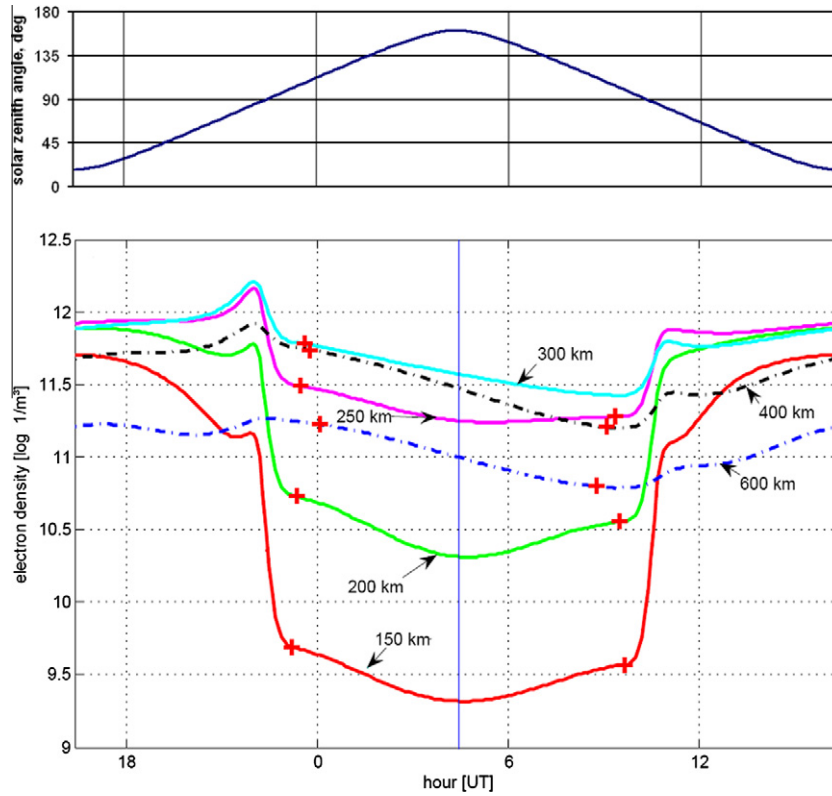


Fig. 2. Idealised diurnal variation of electron densities according to the empirical model built from the Arecibo incoherent scatter radar data (Fankhauser, 2010). The simulation is for spring equinox and otherwise median geophysical conditions. Full night conditions at the different altitudes prevail between the red +.

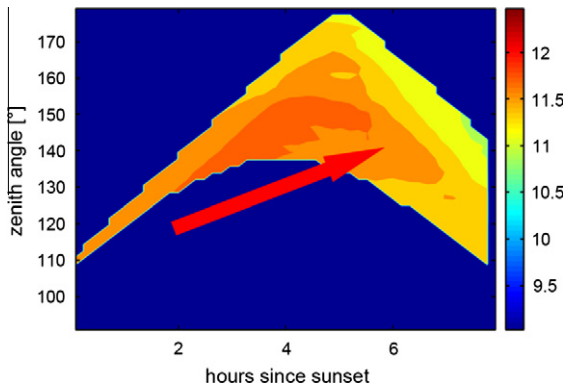


Fig. 3. Electron densities as a function of time after sunset and solar zenith angle at 400 km (Arecibo). Note the seasonal variation of the maximum zenith angle from 140° to 180° and the time from sunset to midnight ranging from 4 to 5 h. The gradient (arrow) with time (h) and zenith angle (deg) after sunset is obtained from an rms-plane fitted to the data.

For the corresponding exercise with the polar cap data we have additional rocket data from Heiss Island and thus also cover lower altitudes. However the data exhibit a much smaller day/night ratio due to the smaller range of zenith angles (median for daytime 91.2°, and 109.7° for night). Here we chose February 1 (rather than equinox) in order that all altitudes considered (i.e. 70–800 km) undergo a day–night variation. The resulting dependences

are much less pronounced than the ones for Arecibo which we attribute to the much longer polar nights when the “orderly” decaying electron densities are superimposed by erratically occurring enhancements due to particle precipitation characteristic for these latitudes. Also the zenith angle between dusk and dawn only covers a few degrees and a dependence is therefore similarly problematic to extract; hence we have to assume that the conclusions pertaining to decay time constants and scattered light dependence obtained from the Arecibo data also apply at the high latitude of EISCAT Svalbard and Heiss Island (78.2° and 80.6°, respectively).

3. Lead time for geophysical parameters

The state of the ionosphere obviously depends on the geophysical parameters at the time, but is also a function of the “geophysical history” preceding that time. Not least the season is such a parameter, *via* the temperature or neutral composition which seasonally varies due to e.g. the different length of the day. Because the lifetime of free electrons at low altitudes is short, one also tends to ignore the conditions prior to the time under investigation. An exception in the *D*-region are the so-called storm after-effects where the ionosphere shows the typical variation controlled by the solar zenith angle, albeit at enhanced electron densities. This enhancement was attributed by

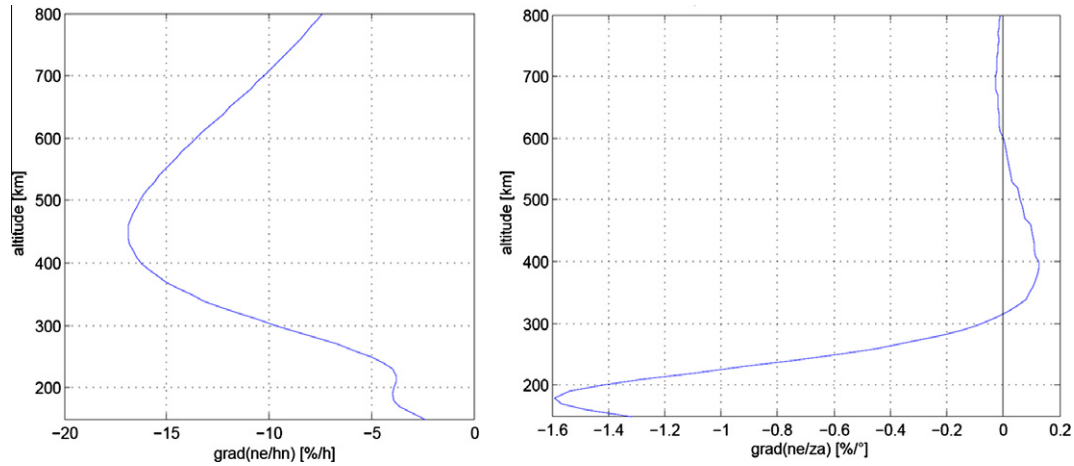


Fig. 4. Electron density decay as a function of time after sunset (in % per hour, left panel) and variation with solar zenith angle beyond sunset (in % per deg, right panel) as a function of altitude. These gradients are derived from the neural network model for median geophysical conditions and spring equinox (Arecibo; cf. Fig. 2).

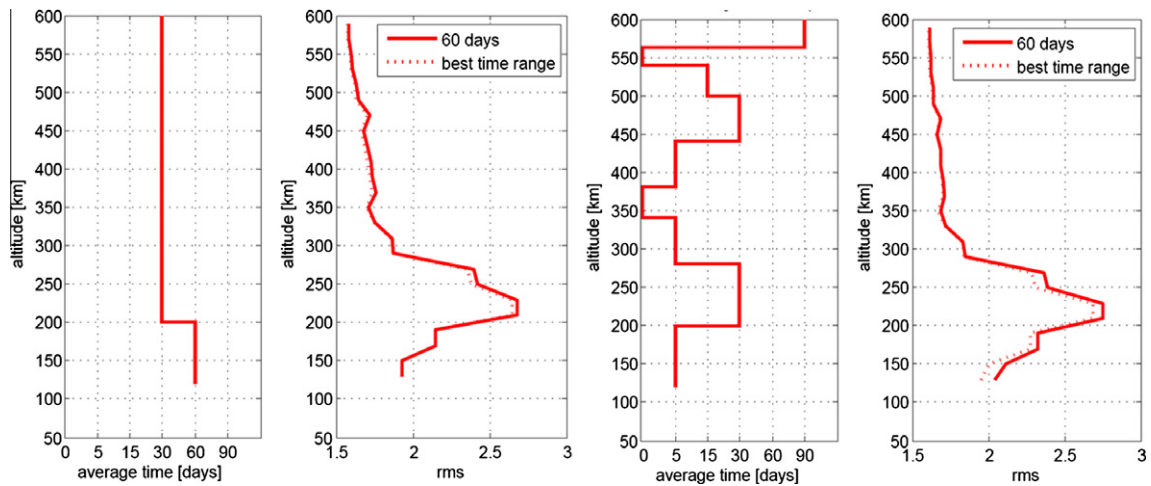


Fig. 5. Influence of the optimal lead-time and the resulting rms-error factors due to varying lead times of the solar flux (left panels) and the magnetic index *ap* (right panels) for predicting electron densities with the Arecibo model. Except for the height region below 200 km generally an average lead time of 30 days yields the smallest rms error factor due to the solar activity lead time; the best lead time for *ap* is more structured with height.

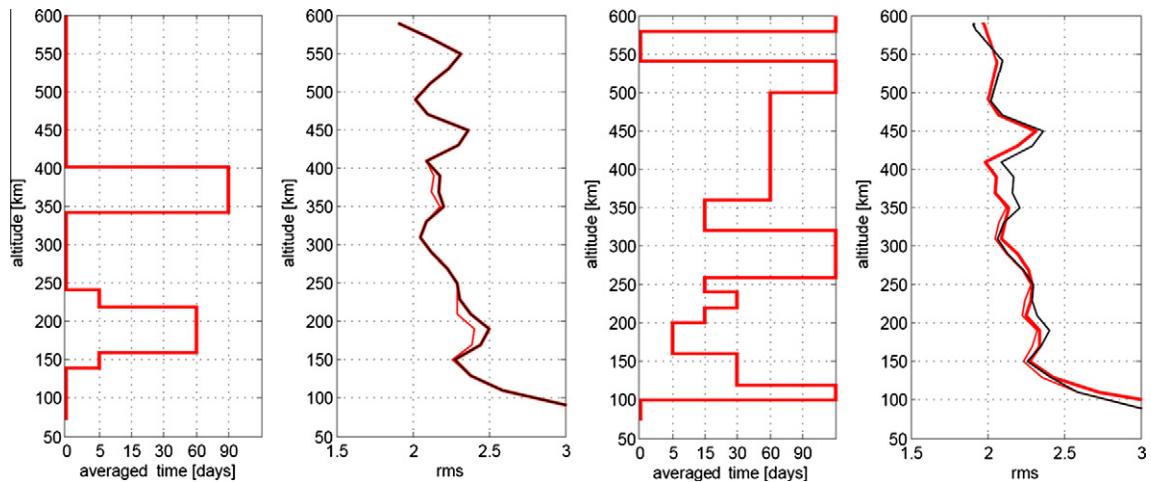


Fig. 6. As Fig. 5, but for Svalbard/Heiss Island steady-state NN model (lead-time = 0), thin red line: optimum lead times in each height interval, bold red lines: 60 day lead time. (For interpretation of the references to colour in this figure legend, the reader is referred to the web version of this article.)

Dickinson and Bennett (1978) to increased nitric oxide densities, in turn due to a particle event the day before. A similar after-effect was found in a correlation analysis of riometer absorption in Greenland and A3 (oblique incidence) radio wave absorption in central Europe (Torkar et al., 1980).

Since at higher altitudes the lifetime of free electrons is longer, one is inclined to also consider the impact of the geophysical conditions prior to the time one investigates or wants to predict. But also the neutral atmosphere is subject to the conditions prevailing in the time before which is e.g. considered in the empirical atmospheric model MSIS (Hedin, 1991). MSIS uses the three-month average of the solar flux ($F_{10.7}$) and the geomagnetic disturbance (ap) of up to 90 hours prior to the time of the prediction. For this test the NN's were thus not only trained with the geophysical condition at the time of the prediction, but also with averaged values of $F_{10.7}$ and ap up to 120 days before the time of the prediction; in these tests the magnetic activity (ap) turned out to be more important than the solar activity ($F_{10.7}$). This lead-time was only varied in coarse steps for best rms error factors (measured values *vs.* corresponding model result) separately every 30 km in altitude (Fig. 5). A constant value of 60 days was found to represent an acceptable compromise which can be used for both locations (Arecibo and Svalbard), all altitudes, and both for ap and $F_{10.7}$ (*cf.*, Fig. 6).

4. Conclusions

After sundown the night-time ionosphere decays exponentially. Below about 200 km the flux of scattered UV introduces a dependence on solar zenith angle and leads to an additional variation symmetric to local midnight. At greater heights the lifetime of free electrons is long

enough such that their exponential decay of typically 10% per hour dominates whereas the zenith angle dependence becomes negligible. In our dataset the geophysical history controlling the electron densities ($F_{10.7}$, ap) is most relevant when averaged over 60 days *prior* to the time under investigation. The results of present preliminary analysis appear reasonable and promising and may stimulate the search for similar behaviour in other ionospheric data.

References

- Dickinson, P.H.G., Bennett, F.D.G. Diurnal variation in the D-region during a storm after-effect. *J. Atmos. Terr. Phys.* 40 (5), 549–551, 1978.
- Fankhauser, M. Time-dependent models of the polar cap and the low latitude ionosphere, PhD thesis, Graz University of Technology, 2010.
- Hedin, A.E. Extension of the MSIS thermospheric model into the middle and lower atmosphere. *J. Geophys. Res.* 96, 1159–1172, 1991.
- Kazil, J. The University of Bern atmospheric ion model: time-dependent ion modelling in the stratosphere, mesosphere and lower thermosphere, PhD Thesis, University of Bern, 2002.
- Ogawa, T., Shimazaki, T. Diurnal variation of odd nitrogen and ionic densities in the mesosphere and lower thermosphere: simultaneous solution of photochemical-diffusive equations. *J. Geophys. Res.* 80, 3945–3960, 1975.
- Sharma, Shweta, Dashora, N., Galav, P., Pandey, R. Total solar eclipse of July 22, 2009: Its impact on the total electron content and ionospheric electron density in the Indian zone. *J. Atmos. Solar Terr. Phys.* 72, 1387–1392, 2010.
- Stauning, P. High-latitude D- and E-region investigations using imaging riometer observations. *J. Atmos. Terr. Phys.* 58 (6), 765–783, 1996.
- Strobel, D.F., Young, T.R., Meier, R.R., Coffey, T.P., Ali, A.W. The nighttime ionosphere: E-region and lower F-region. *J. Geophys. Res.* 79, 3171–3178, 1974.
- Torkar, K.M., Friedrich, M., Stauning, P. Evidence of coupling between auroral zone activity and mid-latitude absorption. *J. Atmos. Terr. Phys.* 42 (2), 183–188, 1980.
- Zell, A., Mamier, G. Stuttgart Neural Network Simulator. University of Stuttgart, 2005.